*Proc. Natl. Acad. Sci. USA*
Vol. 89, pp. 11764–11768, December 1992
Biophysics

# Domain motions in phosphoglycerate kinase: Determination of interdomain distance distributions by site-specific labeling and time-resolved fluorescence energy transfer

**(domain closure/hinge bending/site-directed mutagenesis/emission anisotropy/global analysis)**

G. HARAN*†, E. HAAS*, B. K. SZPIKOWSKA‡, AND M. T. MAS‡§

*Bar-Ilan University, Ramat-Gan 52900, Israel; †Weizmann Institute of Science, Rehovot 72400, Israel; and ‡Beckman Research Institute of the City of Hope, Duarte, CA 91010

*Communicated by Eugene Roberts, August 25, 1992 (received for review May 10, 1992)*

ABSTRACT **3-Phosphoglycerate kinase is composed of two globular domains separated by a wide cleft. The substrate binding sites are situated on the inner surfaces of the two domains. By analogy to other kinases, it has been postulated that the catalytic mechanism of phosphoglycerate kinase involves a hinge bending domain motion that brings the substrates together to allow phosphoryl transfer. To characterize this large-scale conformational change, as well as the dynamics of the unliganded enzyme in solution, we have applied site-directed mutagenesis and time-resolved nonradiative energy transfer techniques. Two genetically engineered cysteines (Cys-135 and Cys-290), one in each of the two domains, were covalently labeled with a donor and acceptor pair of fluorescent probes. Analysis of subnanosecond fluorescence decay curves yielded the equilibrium distribution of interdomain distances. In the absence of substrates, the distribution of distances between the two labeled sites was very broad, with a full width at half maximum estimated as 20 Å or broader, indicative of a large number of conformational substates in solution. The mean distance, 31.5 ± 1 Å, was 8 Å smaller than in the crystal structure. Upon addition of ATP alone or of ATP and 3-phosphoglycerate, the average distance increased to 38 ± 1 Å and the width of the distribution decreased. Addition of 3-phosphoglycerate alone induced a similar but smaller change. The rate of conformational state fluctuations (interconversion between states) was found to be slow on the nanosecond time scale, as expected for a protein with a relatively large interdomain contact area.**

The structures of several kinases determined by x-ray crystallography consist of two distinct domains separated by a deep cleft (1, 2). It has been proposed that a hinge bending domain movement may play an important role in the catalytic mechanism of kinases and other proteins (1–3). The resulting closure of the active-site cleft may be important for bringing together and properly orienting the substrates for phosphoryl transfer and for creating an appropriate anhydrous microenvironment to prevent ATP hydrolysis (1).

3-Phosphoglycerate kinase (PGK) catalyzes a reversible transfer of a phosphoryl group from 1,3-bisphosphoglycerate to ADP in the glycolytic pathway. The crystal structures of the substrate-free enzyme and its binary complex with ATP have been determined for horse muscle (4) and yeast (5) PGKs and represent an "open" conformation. The distance between the γ-phosphate of ATP bound to the C-terminal domain is >10 Å away from the 3-phosphoglycerate (3-PG) binding site situated on the N-terminal domain. This distance is reduced to ≈7.2 Å in the binary complex of pig muscle PGK with 3-PG (6). This decrease and an accompanying domain movement consisting of a 7.7° rotation of the two domains are smaller than predicted for the ternary complex (1, 7).

Evidence for a substrate-induced conformational change in PGK has been obtained from small-angle x-ray scattering experiments in solution that demonstrated a decrease in the radius of gyration ($R_g$) of ≈1 Å for the ternary complex with ATP and 3-PG (8–10). This decrease was found to be consistent with a theoretical model that assumes a hinge-bending rigid body domain motion (8). Site-directed mutagenesis experiments suggested the importance of the structural elements of the hinge region for the transmission of substrate-induced conformational changes in yeast PGK (11–13). Although they provided additional support for the hinge-bending hypothesis, the methods used in these studies were not capable of characterizing the dynamics of conformational fluctuations of PGK in solution.

In this paper we have combined genetic engineering to create specific labeling sites for fluorescent probes and time-resolved fluorescence energy transfer measurements (14–17) to study the conformational flexibility of yeast PGK. This manuscript describes a set of experiments designed to probe the equilibrium conformations of PGK in solution and the effect of added substrates on the conformational state of the enzyme.

## METHODS

**Site-Specific Mutagenesis.** Oligonucleotide-directed mutagenesis of yeast PGK was carried out as described (18). The single cysteine at position 97 of wild-type PGK was mutated to a serine (C97S). Two single-cysteine mutants, (C97S, Q135C)PGK and (C97S,S290C)PGK, and the double-cysteine mutant (C97S,Q135C,S290C)PGK were constructed using the same method.

**Protein Purification and Characterization.** PGK mutants were expressed in *Saccharomyces cerevisiae* XSB44-35D, which lacks PGK, and purified as described (11, 12, 19). DL-Dithiothreitol (DTT; 1 mM) was included in the buffer to minimize thiol oxidation during the purification procedure and during subsequent experiments. Specific activities of the mutant enzymes were measured as described (12). The specific activities of the mutants were similar to the activity of wild-type PGK in the absence and in the presence of activatory sulfate ions, indicating that the mutations do not affect enzyme activity or its activation by sulfate ions.

**Modification of Single Cysteines in (C97S,Q135C)PGK and (C97S,S290C)PGK Mutants with 5-[2-(2-Iodoacetamido)ethylamino]-1-naphthalenesulfonic acid (IAEDANS).** Covalent

The publication costs of this article were defrayed in part by page charge payment. This article must therefore be hereby marked "*advertisement*" in accordance with 18 U.S.C. §1734 solely to indicate this fact.

Abbreviations: IAEDANS, 5-[2-(2-iodoacetamido)ethylamino]-1-naphthalenesulfonic acid; IAF, 5-iodoacetamidofluorescein; PGK, phosphoglycerate kinase; 3-PG, 3-phosphoglycerate; D, fluorescence donor; A, fluorescence acceptor; DTT, dithiothreitol.

§To whom reprint requests should be addressed.

modification of single cysteine residues was carried out at pH 8.0 in 10 mM Hepes containing 1 mM EDTA (buffer H). IAEDANS (fluorescence donor, D) was dissolved in dimethyl formamide (40 mM stock solution). Protein samples (1 mg/ml) were incubated with 20-fold molar excess of IAEDANS for 1 h in the dark. A 10-fold molar excess of DTT over the molar concentration of IAEDANS was then added to stop the reaction, and incubation was continued for 1 h. The unbound probe was then separated by gel filtration on Ultrogel AcA202 (IBF Biotechnics), equilibrated with 10 mM Mops (pH 7.5) containing 1 mM EDTA and 1 mM DTT (buffer M), followed by dialysis against the same buffer. The covalently labeled protein (D-PGK) was separated from unlabeled protein on a DEAE-cellulose (DE-52) column (12 cm × 1.5 cm) equilibrated with buffer M. Two protein peaks were eluted with this buffer. The first peak contained unlabeled protein and was well separated from the second peak, which contained protein covalently labeled with IAEDANS.

**Modification of Single Cysteines in (S97C,Q135C)PGK and (S97C,S290C) Mutants with 5-Iodoacetamidofluorescein (IAF).** IAF, dissolved in dimethylformamide (20 mM stock solution), was added to the protein solution (1 mg/ml) in buffer H, to a final concentration corresponding to a 40-fold molar excess of the reagent over the molar protein concentration. The reaction mixture was incubated in the dark for 4 h at 4°C. The reaction was then quenched with 10-fold molar excess of DTT (over IAF concentration). Free IAF (fluorescence acceptor, A) was separated by gel filtration, followed by an extensive dialysis against buffer M. The covalently labeled protein (A-PGK) was separated from the unlabeled protein by DEAE-cellulose column chromatography. The protein sample was loaded onto a DEAE-cellulose column previously equilibrated with buffer M. The unlabeled protein was eluted with buffer M. The labeled protein species were well-separated using a linear salt gradient elution (0–0.25 M KCl).

**Modification of Cys-135 and Cys-290 in the (C97S,Q135C, S290C)PGK Mutant with IAEDANS and IAF.** The labeling was carried out by one of two methods.

*Method 1.* A sample of (C97S,Q135C,S290C)PGK in buffer H was first incubated with IAEDANS. After separation of the noncovalently bound probe, the sample was modified with IAF. The conditions of chemical modifications and of subsequent separation of free and noncovalently bound reagents were as described above. The dialyzed sample was then subjected to DEAE-cellulose chromatography, as described above. In this protocol, the species labeled with two probes (D-PGK-A) were separated from other species (SH-PGK-SH, D-PGK-SH, D-PGK-D, A-PGK-SH, and A-PGK-A) in a single step.

*Method 2.* Alternatively, after labeling with IAEDANS, the species labeled with 1 mol of IAEDANS per mol of protein (D-PGK-SH) were separated by DEAE-cellulose column chromatography from the unlabeled protein and from protein labeled with two molecules of IAEDANS per molecule of protein (D-PGK-D) prior to labeling with the second probe (IAF). Conditions of labeling with IAF and separation on DEAE-cellulose were the same as described above. After labeling with IAF, the reaction mixture was again subjected to DEAE-cellulose column chromatography.

Prior to the determination of protein concentration, specific activity, and the extent of modification, the samples were concentrated using an Amicon ultrafiltration cell equipped with a Diaflo YM10 membrane. Centricon-30 microconcentrators (Amicon) were used to exchange the buffer to 20 mM triethanolamine acetate (pH 7.5) containing 1 mM DTT, by diafiltration. Stoichiometry of labeling with IAF and IAEDANS was determined spectrophotometrically, using molar extinction coefficients of 71,000 $M^{-1}\cdot cm^{-1}$ at 492 nm and 6100 $M^{-1}\cdot cm^{-1}$ at 337 nm, respectively. Protein concentrations were determined by the method of Bradford (20).

The specific activity of the final sample (A-PGK-D) prepared by either of these two methods was the same as that of an unlabeled control subjected to identical procedures. The net activity loss for the final samples (A-PGK-D and SH-PGK-SH) did not exceed 30%.

**Spectroscopic Methods.** Corrected fluorescence spectra were obtained with a Greg photon-counting spectrofluorometer (I.S.S., Urbana, IL), equipped with a 300-W xenon arc lamp. Time-resolved fluorescence with subnanosecond resolution was measured either on an Edinburgh Instruments (EI, Edinburgh) model 199 time-correlated single-photon counter, equipped with a gas-discharge pulse lamp (21), or on a homemade laser-based time-resolved fluorometer. The latter will be described in detail elsewhere (D. S. Gottfried and E.H., unpublished data). The temperature of the measurements was 4°C. Anisotropy decay measurements were carried out on the EI spectrofluorometer, using Glan–Thomson polarizers. The radiative lifetime of the donor, 45 ns, was determined from measurements of the lifetime and quantum yield of IAEDANS in a buffered aqueous solution (pH 7). The quantum yield was calculated relative to that of a solution of quinine sulfate (5 $\mu$M in 2 M $H_2SO_4$), taken to be 0.7 (22).

## DATA ANALYSIS

The rate of nonradiative energy transfer $k_{ET}$ was calculated according to Förster (14). It is pertinent to note that $k_{ET}$ does not depend on the fluorescence quantum yields and lifetimes of the donor species. This is especially useful in the analysis of experiments in which the donor probe decays with more than one rate constant. Therefore, we used $k_{ET}$ instead of the common analysis, which uses the Förster distance, $R_0$, corresponding to 50% efficiency of energy transfer (14). The average $k_{ET}$ is equivalent to an $R_0$ value of 46 Å, which is close to the crystallographically determined distance between the $\alpha$-carbons of the labeled residues (40 Å).

In the analysis of a time-resolved measurement of energy transfer (16), the dynamics of the excited state of the fluorescent donor are modeled by a one-dimensional reactive diffusion equation (23),

$$\frac{\partial p_i(r,t)}{\partial t} = D\frac{\partial}{\partial r}\left\{e^{-u(r)}\frac{\partial}{\partial r}[e^{u(r)}p_i(r,t)]\right\} - k(r)p_i(r,t). \quad [1]$$

In this equation, $p_i(r, t)$ is the probability density of finding an excited state donor species with distance $r$ from the acceptor at time $t$ after excitation, so that the total probability density is $p(r, t) = \Sigma_i\, p_i(r, t)$. $D$ is the intramolecular diffusion constant, and $u(r)$ is a distance-dependent potential of mean force in $k_BT$ units ($k_B$, Boltzmann constant; $T$, temperature). This potential is usually taken to be harmonic (thus implying a Gaussian distribution for the distance between the fluorescent probes): $u(r) = a(r - b)^2$, where $a$ and $b$ are parameters. $k(r)$ is the reaction term including the Förster energy-transfer rate and the spontaneous emission rate.

Decay curves were calculated from the solutions of Eq. 1 (23) and fitted to the experimental data by using a modified version of GLOBAL (23–25).

Anisotropy decay measurements were analyzed using the vector method (26). The anisotropy decay $r(t)$ was fitted to the following function

$$r(t) = r_0[(1 - \alpha)e^{-t/\phi_1} + \alpha]e^{-t/\phi_2}, \quad [2]$$

where $r_0$ is the limiting anisotropy (measured independently using glycerol solutions of the labeled proteins), $\phi_1$ and $\phi_2$ are rotational correlation times, and $r_0 \times \alpha$ is the equivalent of $r_\infty$

of Kinosita *et al.* (27), from which the cone angle of a hindered rotator, $\theta_{max}$, can be calculated.

The goodness of fit criteria and error intervals for fitting parameters were computed by the rigorous analysis procedure (23, 28).

## RESULTS

**Design of Labeled Derivatives.** Site-directed mutagenesis was used to introduce cysteine residues suitable for subsequent labeling with pairs of fluorescent thiol-reactive probes (donor and acceptor of excitation energy). Only surface-exposed polar residues were selected for mutagenesis to minimize possible perturbations of PGK structure and function (due to the mutagenesis and/or chemical modification) and to increase the probability that covalently bound probes will rotate freely. The naturally occurring cysteine in yeast PGK was replaced with serine prior to engineering the desired labeling sites.

In this paper we focus on the double cysteine mutant (C97S,Q135C,S290C)PGK and the corresponding single-cysteine mutants (C97S,Q135C)PGK and (C97S,S290C)-PGK. Fig. 1 shows the location of the two labeled sites, Cys-135 and Cys-290, the former in the N-terminal domain and the latter in the C-terminal domain. The distance between the labeling sites was expected to experience maximal change in the proposed hinge-bending motion.

Absorption spectra of the two probes, IAEDANS (D) and IAF (A), and emission spectra of an IAEDANS-labeled mutant (D-PGK) and an IAF-labeled mutant (A-PGK) are shown in Fig. 2.

Various D-PGK mutants had very similar emission spectra. IAEDANS is strongly environment-sensitive (29) and, therefore, the similarity between spectra indicates that the probe is solvated to the same extent in each of the mutants. This result indicates lack of specific interactions between the probe and the protein surface but not necessarily other (nonspecific) interactions with side chains. Indeed, the emission spectrum shows a blue shift with respect to the spectrum of free IAEDANS in water. This shift indicates that the probe experiences a less polar environment or reduced solvent relaxation when covalently bound to PGK. The same trend was found for A-PGK mutants. Since IAF is known to be pH sensitive (30), the spectral similarity indicates a lack of local differences in the proton concentration, thus ruling out local specific interactions.

**Steady-State Anisotropy.** The fluorescence anisotropies ($r$) of each single-labeled mutant (Table 1) were used for estimation of the probable error ranges for the calculated distances arising from the use of an average orientational factor ($\kappa^2$). A comparison of the values reported in Table 1 with values reported in tables II and III of Haas *et al.* (16) shows that an error of <10% in the measured distances is expected in the present experiments. This conclusion is further confirmed by the observation that ATP binding (data not shown) does not change $r$ and by anisotropy decay measurements (see below).

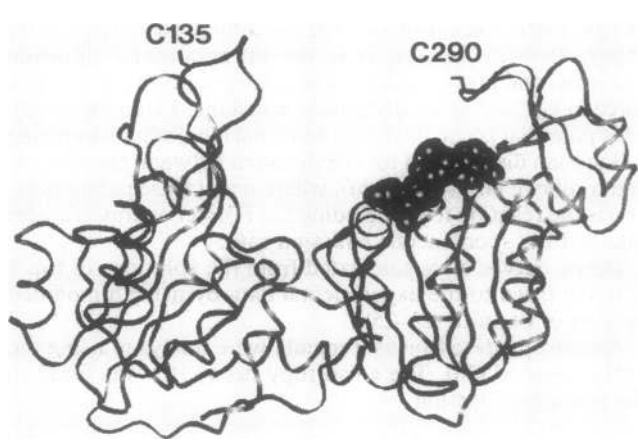


FIG. 1. Schematic representation of the crystal structure of yeast PGK with bound ATP (5). Two cysteines, labeled C135 and C290, were introduced by site-directed mutagenesis to create specific labeling sites for fluorescent probes.

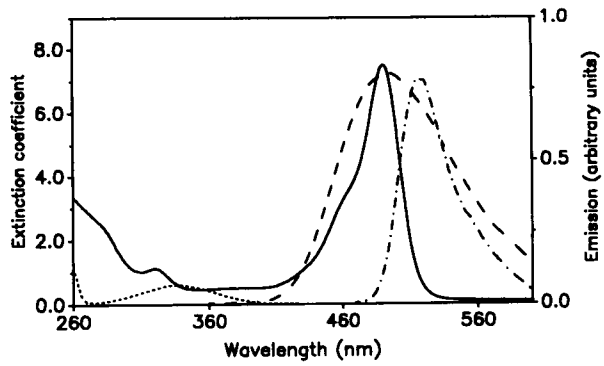


FIG. 2. Absorption spectra of IAEDANS (– – –) and IAF (——) and fluorescence emission spectra of D-PGK (- - -) and A-PGK (– · – ·). The excitation coefficient is presented as $M^{-1}\cdot cm^{-1}$ ($\times 10^{-4}$).

**Fluorescence Decay.** The fluorescence decay of the D-PGK mutants was fitted satisfactorily to a sum of two exponentials (Table 1). The lifetime of the donor is influenced by the site of labeling. This is taken into account in the distribution analysis. In the double-labeled derivative, the probes are distributed between the two sites. This internal averaging reduces possible effects of site-specific interactions. The fluorescence decay of A-PGK mutants was monoexponential in all cases studied (Table 1).

**Anisotropy Decay of IAEDANS-Labeled Mutants.** The existence of a very short correlation time in the anisotropy decay of both D-PGK mutants (Table 2) is consistent with a relatively free rotational motion of the probes on the protein (or fast local segmental motions), as also concluded on the basis of the steady-state anisotropy measurements. By assuming a hindered rotation model (27), we calculated the cone of rotation angles, $\theta_{max}$, for the two mutants (Table 2). The large angles (>40°) are also indicative of the lack of any specific interactions, which might hinder rotational motion of the probe.

**Energy-Transfer Measurements.** Decay data for each sample were collected at four wavelengths (490, 520, 550, and 580 nm). Since the emission and absorption spectra of the donor and the acceptor overlap, each experimentally observed decay curve contained (*i*) contributions by both probes and (*ii*) a contribution by direct excitation of the acceptor. The

Table 1. Fluorescence characteristics of single-labeled PGK mutants

| Mutant | Steady-state anisotropy | Emission decay | |
|---|---|---|---|
| | | Lifetime, nsec | Weight |
| D135 | 0.13* | 18.2 (16.5–21.5) | 0.29 (0.15–0.48) |
| | | 11.0 (10.0–11.8) | 0.71 (0.52–0.85) |
| D290 | 0.13* | 27.7 (26.8–29.0) | 0.53 (0.47–0.59) |
| | | 11.6 (10.6–12.7) | 0.47 (0.42–0.53) |
| A135 | 0.24† | 4.03 (4.01–4.05) | — |
| A290 | 0.24† | 3.94 (3.92–3.97) | — |

For steady-state anisotropy, each value is an average of three measurements (error, ±0.01 or less). Values in parentheses represent 1 SD calculated by a rigorous analysis approach.
*Excitation wavelength, 340 nm; emission wavelength, 470 nm.
†Excitation wavelength, 490 nm; emission wavelength, 540 nm.

Table 2. Anisotropy decay of IAEDANS-labeled mutants

| Parameter | Mutant | |
|---|---|---|
| | D135 | D290 |
| $\alpha$ | 0.30 (0.27–0.32) | 0.40 (0.39–0.42) |
| $\theta_{max}$, degrees | 49 | 43 |
| $\phi_1$, nsec | 0.21 (0.12–0.30) | 0.14 (0.0–0.24) |
| $\phi_2$, nsec | 30.0 (24.5–37.0) | 51.0 (45.0–57.0) |

For definition of parameters, see *Data Analysis*. The $r_0$ value used was 0.36. Values in parentheses represent 1 SD confidence interval.

latter was accounted for by addition of a decay component of the free acceptor with a weight based on the ratio of the extinction coefficients of the acceptor and the donor at the excitation wavelength (23). The relative contribution of each probe at each of the four emission wavelengths depends on the quantum yield and the spectral responses of the detection system. These were obtained from measurements of single-labeled protein samples (D-PGK-SH and A-PGK). Those measurements also served as an internal reference in the analysis. The fluorescence decays of D-PGK-SH and of D-PGK-A are shown in Fig. 3. The average lifetime of the D-PGK-A sample was 78% lower than that of the D-PGK-SH sample (the reference derivative), a net effect of the excitation transfer process. When D-PGK-A was unfolded in guanidine hydrochloride, the average lifetime of the donor was only 20% shorter than that of D-PGK-SH. This control experiment confirms the relation between lifetime reduction and donor–acceptor distance.

The fluorescence decay curves of D-PGK-SH and D-PGK-A (the latter measured at four wavelengths) were globally analyzed and the calculated equilibrium interprobe distance distribution was plotted in Fig. 4. The mean and full width at half maximum (FWHM) of the distribution are given in Table 3. The mean interprobe distance, 31.5 ± 1 Å, is lower by ≈8 Å than the crystal structure distance between the $\alpha$-carbons of the labeled residues, 40 Å (5). The distribution

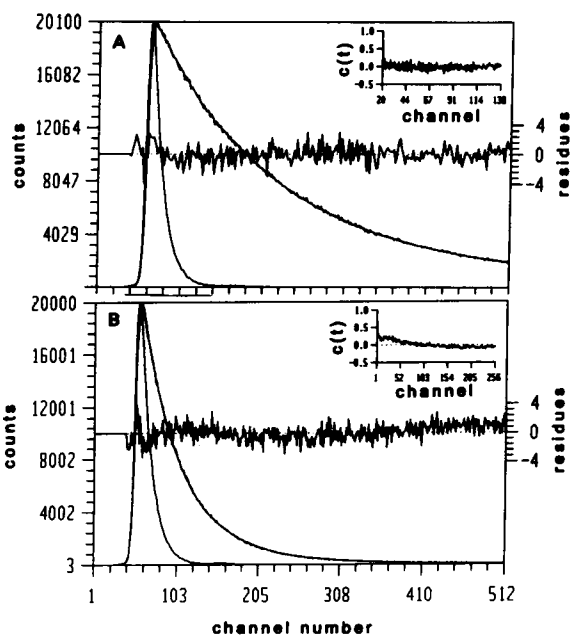


FIG. 3. Comparison of the fluorescence decay of IAEDANS-labeled PGK before (*A*) and after (*B*) subsequent labeling with IAF. A major reduction in the average lifetime is apparent. The narrow pulse is the trace of the fluorescence decay of the reference. The curve in the middle of each figure shows the residuals of the fit. (*Insets*) Autocorrelation of the residuals, c(t). (*A*) Decay was fitted to a double-exponential model. (*B*) Fit is from a detailed energy-transfer analysis.

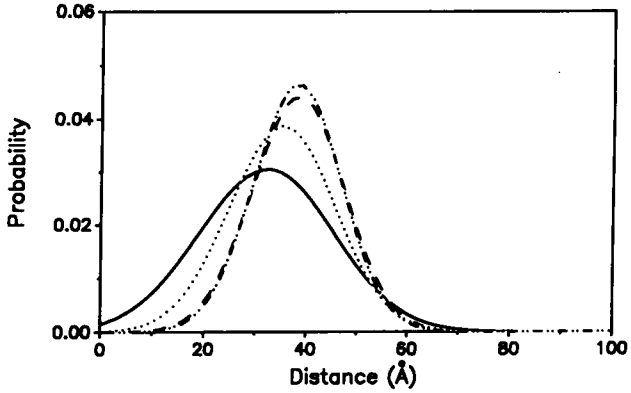


FIG. 4. Interprobe equilibrium distance distribution function without substrates (——), in the presence of ATP (– ·· –), in the presence of 3-PG (· · ·), and in the presence of ATP and 3-PG (– – –).

is very broad, with a FWHM >31 ± 2 Å, suggesting considerable flexibility in the structure of PGK.

An upper bound for the diffusion constant was also obtained from global analysis. We found that any value between zero and $1 \times 10^{-7}$ cm$^2$/sec gave a satisfactory fit to the data. This result indicates that the rate of conformational state interconversion in PGK is small on the time scale of our measurements.

Similar sets of measurements and analyses were carried out in the presence of Mg-ATP, 3-PG, or both substrates (each in a concentration of 10 mM; Table 3). The main, and surprising, result of this experiment is the observation that ATP binding caused an increase of the mean interprobe distance by ≈7 ± 1 Å, while narrowing the width of the distance distribution. This result was consistently reproduced in several different sets of measurements using several different preparations and is thus beyond experimental uncertainty. The addition of 3-PG induced a smaller change of the interprobe distance, which was increased to ≈35 ± 1 Å. In the presence of both substrates the mean interprobe distance was approximately the same as in the presence of ATP alone.

## DISCUSSION

The main result of our experiments and analysis is the determination of the distribution of distances between the labeled sites on the two domains of PGK. The average interprobe distance in solution was found to be lower than the distance in the crystal structure. Since the probes are attached to the protein by flexible side chains, possible influence of the conformation of the probes' side chains on the calculated distances should be considered. The fast anisotropy decay rate component (Table 2) and the low steady-state anisotropy values (Table 1) indicate free rotation of the probes and thus rule out contribution of possible biased probe orientations to the measured distance. However, the contribution of conformational flexibility of the labeled chain segments (loops) to the measured distance cannot be ruled out in the present experiment. The average conformation of these loops in solution can conceivably be different than the

Table 3. Distance distribution parameters

| Substrate(s) | Mean distance, Å | FWHM, Å |
|---|---|---|
| None | 31.5 (31.0–32.0) | 31.4 (29.4–33.9) |
| + ATP | 38.3 (37.9–38.7) | 21.1 (19.9–23.5) |
| + 3-PG | 35.2 (34.6–35.6) | 24.2 (23.0–25.6) |
| + ATP + 3-PG | 38.2 (37.7–38.6) | 20.2 (18.8–21.5) |

Data in parentheses are 1 SD error levels. FWHM, full width at half maximum of the distribution.

conformation observed in the crystal structure. Complementary measurements using a series of PGK mutants labeled at additional pairs of sites, as well as with different probes, are needed to provide a comprehensive description of the relative motions of individual elements of the structure. With all this in mind, we interpret the above results as indicative of the fact that in solution the mean interdomain distance in yeast PGK, measured between residues 135 and 290, is smaller than that found in the crystal.

The width of the distribution includes a contribution from the conformational distribution of the side chains of the probes. The latter was qualitatively assessed by the method of McWherter *et al.* (31), using the rotational isomer state model of Flory (32). Details of the calculations for the present case will be given elsewhere. Based on these calculations, we estimate that the true width of the distance distribution between residues 135 and 290 in yeast PGK in solution at 4°C is ≈20 Å. This result indicates that in solution PGK may assume a wide range of conformational substates. The increase of the mean interdomain distance after addition of the substrates is a further indication of the importance of conformational flexibility in PGK. This increase could conceivably occur as the result of a hinge bending motion that involves a relative rotation of the two domains, which effectively increases the distance between Cys-135 and Cys-290. Alternatively, or in addition to a hinge-bending motion, the substrate-induced conformational changes may lead to propagated conformational transitions that involve structural elements inside one or both domains and give rise to an outward motion of the loops to which the probes are attached. The concomitant narrowing of the distance distributions also indicates changes in the conformational equilibrium of the enzyme in the presence of substrates.

The calculated intramolecular diffusion constant is smaller than $10^{-7}$ $cm^2/sec$. This indicates that the rate of interconversion between conformational substates is slow on the nanosecond time scale. A slow rate of interconversion is expected based on the relatively large interdomain contact area, which requires multiple rearrangements at the interface to accommodate hinge bending domain motions.

The introduction of cysteines into PGK and subsequent labeling with fluorescent probes does not seem to cause significant perturbation in the enzyme structure or function. The activity of the unlabeled mutants is virtually identical to the activity of wild-type PGK. Although the activity of the labeled enzyme was reduced by ≈30% relative to untreated enzyme, we have shown that this reduction is not due to the attachment of extrinsic probes but is due to the long preparative process. It should be noted that enzyme activity is very sensitive to minor local changes (e.g., side chain conformations). It has been shown (33) that the activity loss in PGK, observed at low denaturant concentrations, occurs in the absence of changes in physical signals (CD and fluorescence) that are sensitive to changes in the secondary and tertiary structure. It is possible that the width determined by the current experiments is somewhat larger than what would be found in a nontreated enzyme.

In conclusion, we have shown that the solution structure and dynamics of the bidomain enzyme PGK are different from what could be predicted from the crystal structure alone. The mechanism of action of PGK, which appears to require structural flexibility, is likely to involve a series of interdomain and intradomain conformational changes.

We thank Drs. E. Katchalski-Katzir, I. Z. Steinberg, H. A. Scheraga, and O. B. Ptitsyn for illuminating discussions. The contribution of Dr. D. S. Gottfried and the technical assistance of Mr. D. Friedman are gratefully acknowledged. We thank Dr. M. A. Sherman for preparation of Fig. 1 and for critical reading of the manuscript. We also thank Dr. Nancy L. McQueen for her contribution in the early stage of this project. This work was supported by National Institutes of Health Grant GM 41360 (to M.T.M. and E.H.) and equipment grants from the Basic Research Fund of the Israeli Academy of Sciences (1984, 1988, and 1990) and from the Russell Foundation of Miami Beach Florida (to E.H.).

1. Anderson, C. M., Zucker, F. H. & Steitz, T. A. (1979) *Science* **204**, 375–380.
2. Bennet, W. S. & Huber, R. (1983) *CRC Crit. Rev. Biochem.* **15**, 291–384.
3. Schulz, G. E. (1991) *Curr. Opinion Struct. Biol.* **1**, 883–888.
4. Banks, R. D., Blake, C. C. F., Evans, P. R., Haser, R., Rice, D. W., Hardy, G. W., Merrett, M. & Phillips, A. W. (1979) *Nature (London)* **279**, 773–777.
5. Watson, H. C., Walker, N. P. C., Shaw, P. J., Bryant, T. N., Wendell, P. L., Fothergill, L. A., Perkins, R. E., Conroy, S. C., Dobson, M. J., Tuite, M. F., Kingsman, A. J. & Kingsman, S. M. (1982) *EMBO J.* **1**, 1635–1640.
6. Harlos, K., Vas, M. & Blake, C. F. (1992) *Proteins* **12**, 133–144.
7. Blake, C. C. F., Rice, D. W. & Cohen, F. E. (1986) *Int. J. Pept. Protein Res.* **27**, 443–448.
8. Pickover, C. A., McKay, D. B., Engelman, D. M. & Steitz, T. M. (1979) *J. Biol. Chem.* **22**, 11323–11329.
9. Timchenko, A. A. & Tsyuryupa, S. N. (1982) *Biophysics* **27**, 1065–1069.
10. Sinev, M. A., Razgulyaev, O. I., Vas, M., Timchenko, A. A. & Ptitsyn, O. B. (1989) *Eur. J. Biochem.* **180**, 61–66.
11. Mas, M. T., Resplandor, Z. E. & Riggs, A. D. (1987) *Biochemistry* **26**, 5369–5377.
12. Mas, M. T., Bailey, J. M. & Resplandor, Z. E. (1988) *Biochemistry* **27**, 1168–1172.
13. Mas, M. T. & Resplandor, Z. E. (1988) *Proteins* **4**, 56–62.
14. Förster, T. (1948) *Ann. Phys. (Leipzig)* **2**, 55–75.
15. Stryer, L. (1978) *Annu. Rev. Biochem.* **47**, 819–846.
16. Haas, E., Katchalski-Katzir, E. & Steinberg, I. Z. (1978) *Biochemistry* **17**, 5064–5070.
17. Amir, D. & Haas, E. (1987) *Biochemistry* **26**, 2162–2175.
18. Sherman, M. A., Szpikowska, B. K., Dean, S. A., Mathiowetz, A. M., McQueen, N. L. & Mas, M. T. (1990) *J. Biol. Chem.* **265**, 10659–10665.
19. Mas, M. T., Chen, C. Y., Hitzeman, R. A. & Riggs, A. D. (1986) *Science* **233**, 788–790.
20. Bradford, M. M. (1976) *Anal. Biochem.* **72**, 248–254.
21. Birch, D. J. S. & Imhof, R. E. (1981) *Rev. Sci. Instrum.* **52**, 1206–1212.
22. Scott, T. G., Spencer, R., Leonard, N. & Weber, G. (1970) *J. Am. Chem. Soc.* **92**, 687–695.
23. Beechem, J. M. & Haas, E. (1989) *Biophys. J.* **55**, 1225–1236.
24. Beechem, J. M., Ameloot, M. & Brand, L. (1985) *Chem. Phys. Lett.* **120**, 466–472.
25. Bevington, P. R. (1969) *Data Reduction and Error Analysis for the Physical Sciences* (McGraw–Hill, New York).
26. Gilbert, C. W. (1983) in *Time-Resolved Fluorescence Spectroscopy in Biochemistry and Biology*, eds. Cundall, R. B. & Dale, R. E. (Plenum, New York), pp. 605–606.
27. Kinosita, K., Kawato, S. & Ikegami, A. (1977) *Biophys. J.* **20**, 289–305.
28. Grinvald, A. & Steinberg, I. Z. (1974) *Anal. Biochem.* **59**, 583–598.
29. Hudson, E. N. & Weber, G. (1973) *Biochemistry* **12**, 4154–4160.
30. Ohkuma, S. & Poole, B. (1978) *Proc. Natl. Acad. Sci. USA* **75**, 3327–3331.
31. McWherter, C. A., Haas, E., Leed, A. R. & Scheraga, H. A. (1986) *Biochemistry* **25**, 1951–1963.
32. Flory, P. (1969) *Statistical Mechanics of Chain Molecules* (Interscience, New York).
33. Betton, J.-M., Desmadril, M., Mitraki, A. & Yon, J. M. (1984) *Biochemistry* **23**, 6654–6661.